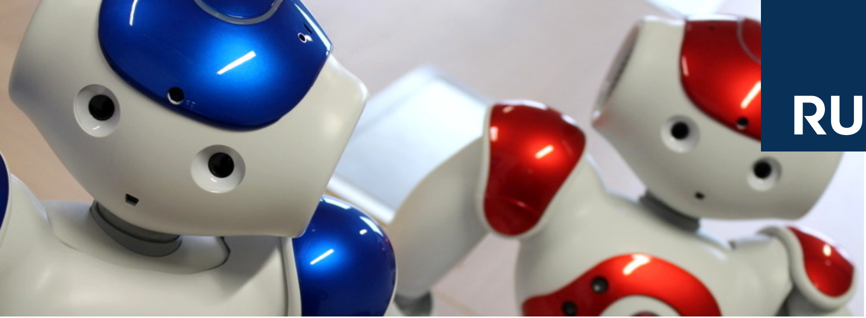

Exploiting Structures of Temporal Causality for Robust Speaker Localization in Reverberant Environments

Christopher Schymura, Peng Guo, Yanir Maymon, Boaz Rafaely, Dorothea Kolossa

July 4th, 2018

RUHR UNIVERSITÄT BOCHUM RUB

Ben-Gurion University of the Negev

Outline

Outline

Introduction

Application domain

- Speaker localization in reverberant rooms.
- Applications: Speech enhancement, teleconferencing, smart home, virtual reality, robot audition, ...
- Active field of research.[1] [2] [3]

[1] N. Ma, G. J. Brown, T. May (2015): *"Exploiting deep neural networks and head movements for binaural localisation of multiple speakers in reverberant conditions"*

[2] X. Li, L. Girin, F. Badeig, R. Horaud (2016): *"Reverberant sound localization with a robot head based on direct-path relative transfer function"*

[3] B. Rafaely, D. Kolossa, Y. Maymon (2017): *"Towards acoustically robust localization of speakers in a reverberant environment"*

Introduction

Application domain

- Speaker localization in reverberant rooms.
- Applications: Speech enhancement, teleconferencing, smart home, virtual reality, robot audition, ...
- Active field of research.[1] [2] [3]

[1] N. Ma, G. J. Brown, T. May (2015): *"Exploiting deep neural networks and head movements for binaural localisation of multiple speakers in reverberant conditions"*

[2] X. Li, L. Girin, F. Badeig, R. Horaud (2016): *"Reverberant sound localization with a robot head based on direct-path relative transfer function"*

[3] B. Rafaely, D. Kolossa, Y. Maymon (2017): *"Towards acoustically robust localization of speakers in a reverberant environment"*

Introduction

Application domain

- Speaker localization in reverberant rooms.
- Applications: Speech enhancement, teleconferencing, smart home, virtual reality, robot audition, ...
- Active field of research.[1] [2] [3]

[1] N. Ma, G. J. Brown, T. May (2015): *"Exploiting deep neural networks and head movements for binaural localisation of multiple speakers in reverberant conditions"*

[2] X. Li, L. Girin, F. Badeig, R. Horaud (2016): *"Reverberant sound localization with a robot head based on direct-path relative transfer function"*

[3] B. Rafaely, D. Kolossa, Y. Maymon (2017): *"Towards acoustically robust localization of speakers in a reverberant environment"*

Introduction

Application domain

- Speaker localization in reverberant rooms.
- Applications: Speech enhancement, teleconferencing, smart home, virtual reality, robot audition, ...
- Active field of research.[1] [2] [3]

[1]N. Ma, G. J. Brown, T. May (2015): *"Exploiting deep neural networks and head movements for binaural localisation of multiple speakers in reverberant conditions"*

[2]X. Li, L. Girin, F. Badeig, R. Horaud (2016): *"Reverberant sound localization with a robot head based on direct-path relative transfer function"*

[3]B. Rafaely, D. Kolossa, Y. Maymon (2017): *"Towards acoustically robust localization of speakers in a reverberant environment"*

Introduction

Localization framework

- Direct-path dominance (DPD) test-based direction-of-arrival (DoA) estimation.[4]
- Clustering of estimated DoAs using a Gaussian mixture model (GMM).[5]
- Speaker DoA determined by selecting the dominant Gaussian component of the GMM.

[4] O. Nadiri, B. Rafaely (2014): *"Localization of Multiple Speakers under High Reverberation using a Spherical Microphone Array and the Direct-Path Dominance Test"*

[5] B. Rafaely, D. Kolossa (2017): *"Speaker localization in reverberant rooms based on direct path dominance test statistics"*

Introduction

Localization framework

- Direct-path dominance (DPD) test-based direction-of-arrival (DoA) estimation.[4]
- Clustering of estimated DoAs using a Gaussian mixture model (GMM).[5]
- Speaker DoA determined by selecting the dominant Gaussian component of the GMM.

[4] O. Nadiri, B. Rafaely (2014): *"Localization of Multiple Speakers under High Reverberation using a Spherical Microphone Array and the Direct-Path Dominance Test"*

[5] B. Rafaely, D. Kolossa (2017): *"Speaker localization in reverberant rooms based on direct path dominance test statistics"*

Introduction

Localization framework

- Direct-path dominance (DPD) test-based direction-of-arrival (DoA) estimation.[4]
- Clustering of estimated DoAs using a Gaussian mixture model (GMM).[5]
- Speaker DoA determined by selecting the dominant Gaussian component of the GMM.

[4] O. Nadiri, B. Rafaely (2014): *"Localization of Multiple Speakers under High Reverberation using a Spherical Microphone Array and the Direct-Path Dominance Test"*

[5] B. Rafaely, D. Kolossa (2017): *"Speaker localization in reverberant rooms based on direct path dominance test statistics"*

Introduction

Localization framework

- Direct-path dominance (DPD) test-based direction-of-arrival (DoA) estimation.[4]
- Clustering of estimated DoAs using a Gaussian mixture model (GMM).[5]
- Speaker DoA determined by selecting the dominant Gaussian component of the GMM.

[4]O. Nadiri, B. Rafaely (2014): *"Localization of Multiple Speakers under High Reverberation using a Spherical Microphone Array and the Direct-Path Dominance Test"*

[5]B. Rafaely, D. Kolossa (2017): *"Speaker localization in reverberant rooms based on direct path dominance test statistics"*

GMM-based DoA clustering

Reverberation time: $T_{60} = 0.5\,\mathrm{s}$

$$\log p(\boldsymbol{\theta} \mid \{\pi_i, \boldsymbol{\mu}_i, \boldsymbol{\Sigma}_i\}_{i=1}^{C})$$

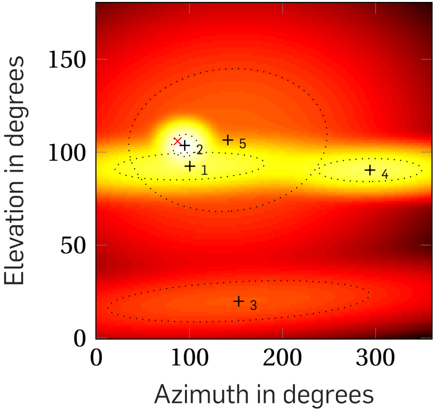

GMM-based DoA clustering

Reverberation time: $T_{60} = 0.5\,\mathrm{s}$

$$\log p(\boldsymbol{\theta} \,|\, \{\pi_i, \boldsymbol{\mu}_i, \boldsymbol{\Sigma}_i\}_{i=1}^{C})$$

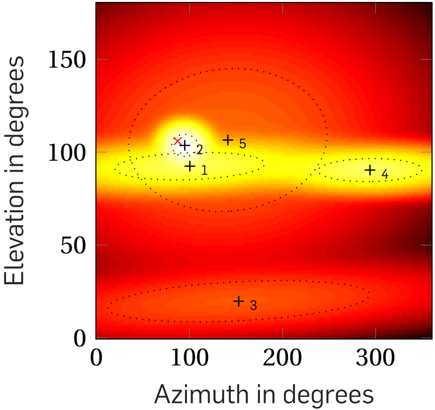

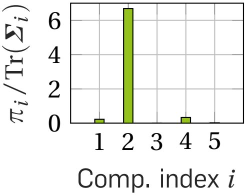

GMM-based DoA clustering

Reverberation time: $T_{60} = 1.0\,\mathrm{s}$

$$\log p(\boldsymbol{\theta} \mid \{\pi_i, \boldsymbol{\mu}_i, \boldsymbol{\Sigma}_i\}_{i=1}^{C})$$

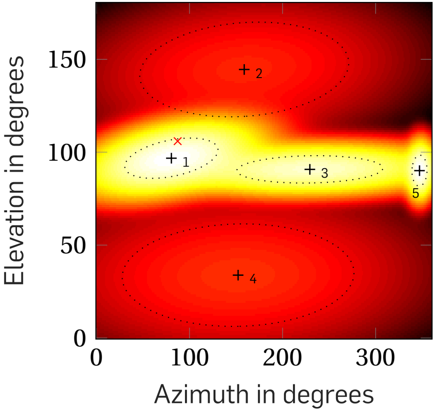

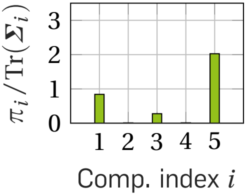

GMM-based DoA clustering

Reverberation time: $T_{60} = 2.0\,\mathrm{s}$

$$\log p(\boldsymbol{\theta} \mid \{\pi_i, \boldsymbol{\mu}_i, \boldsymbol{\Sigma}_i\}_{i=1}^{C})$$

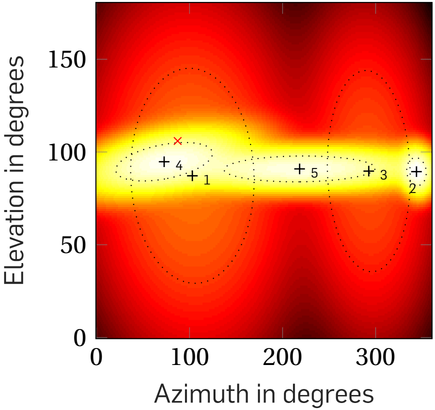

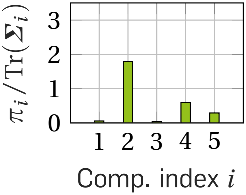

Outline

Temporal structure of RIRs

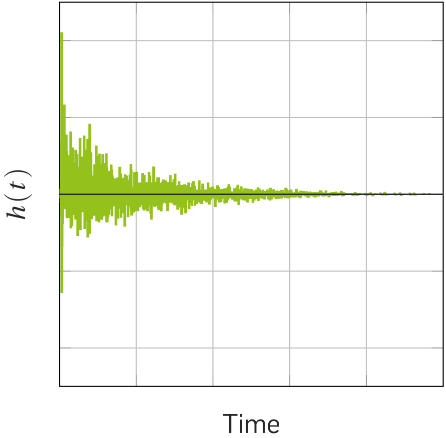

Temporal structure of RIRs

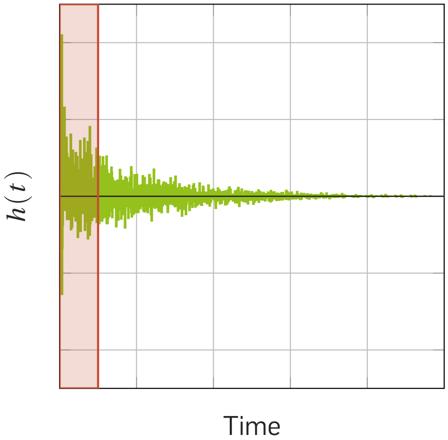

Temporal structure of RIRs

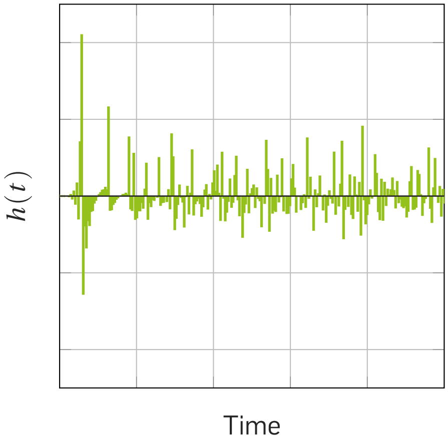

Temporal structure of RIRs

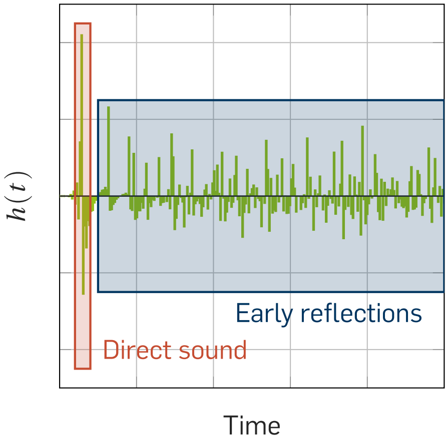

Toy example for time-series modeling

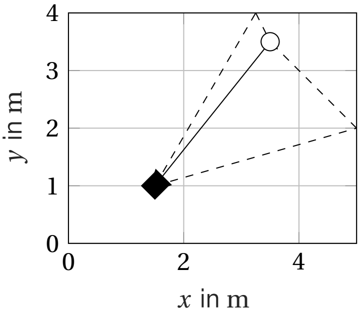

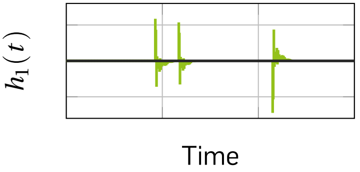

$$\log p(\boldsymbol{\theta} \mid \{\pi_i, \boldsymbol{\mu}_i, \boldsymbol{\Sigma}_i\}_{i=1}^{C})$$

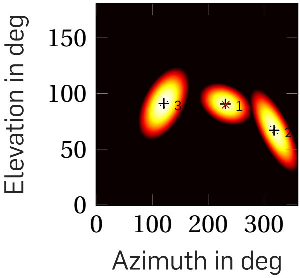

DoA-dependent time-series

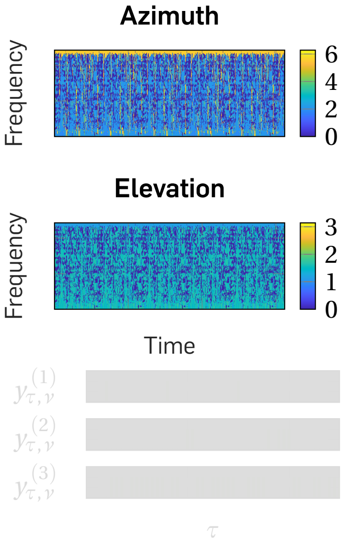

1. Generate DoA time-series for each frequency bin:

$$\boldsymbol{\Theta}_{\nu} = \Big\{ \underbrace{\left[\phi_{\tau,\nu} \quad \psi_{\tau,\nu} \right]^{\mathrm{T}}}_{\boldsymbol{\theta}_{\tau,\nu}^{\mathrm{T}}} \Big\}_{\tau=1}^{T}$$

2. Evaluate component-wise Gaussian posteriors:

$$y_{\tau,\nu}^{(i)} = p(\boldsymbol{\theta}_{\tau,\nu} | \boldsymbol{\mu}_i, \boldsymbol{\Sigma}_i)$$

3. Generate time-series from posteriors:

$$\boldsymbol{y}_{\nu} = \{ y_{\tau,\nu}^{(i)} \}_{\tau=1}^{T}$$

DoA-dependent time-series

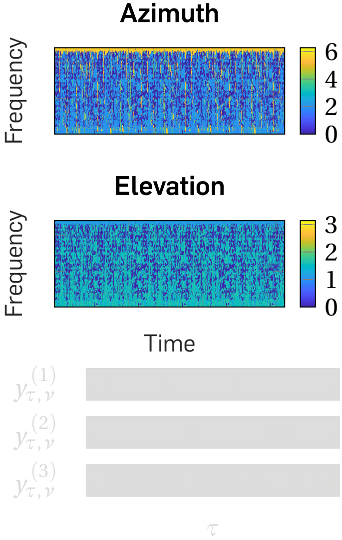

1. Generate DoA time-series for each frequency bin:

$$\boldsymbol{\Theta}_{\nu} = \Big\{ \underbrace{\begin{bmatrix} \phi_{\tau,\nu} & \psi_{\tau,\nu} \end{bmatrix}^{\mathrm{T}}}_{\boldsymbol{\theta}^{\mathrm{T}}_{\tau,\nu}} \Big\}_{\tau=1}^{T}$$

2. Evaluate component-wise Gaussian posteriors:

$$y^{(i)}_{\tau,\nu} = p(\boldsymbol{\theta}_{\tau,\nu} | \boldsymbol{\mu}_i, \boldsymbol{\Sigma}_i)$$

3. Generate time-series from posteriors:

$$\boldsymbol{y}_{\nu} = \{ y^{(i)}_{\tau,\nu} \}_{\tau=1}^{T}$$

DoA-dependent time-series

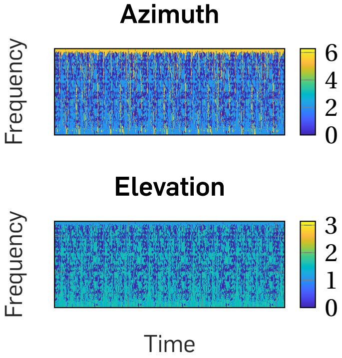

1. Generate DoA time-series for each frequency bin:

$$\boldsymbol{\Theta}_{\nu} = \Big\{ \underbrace{\big[\phi_{\tau,\nu} \quad \psi_{\tau,\nu}\big]^{\mathrm{T}}}_{\boldsymbol{\theta}^{\mathrm{T}}_{\tau,\nu}} \Big\}_{\tau=1}^{T}$$

2. Evaluate component-wise Gaussian posteriors:

$$y_{\tau,\nu}^{(i)} = p(\boldsymbol{\theta}_{\tau,\nu} | \boldsymbol{\mu}_i, \boldsymbol{\Sigma}_i)$$

3. Generate time-series from posteriors:

$$\boldsymbol{y}_{\nu} = \{y_{\tau,\nu}^{(i)}\}_{\tau=1}^{T}$$

DoA-dependent time-series

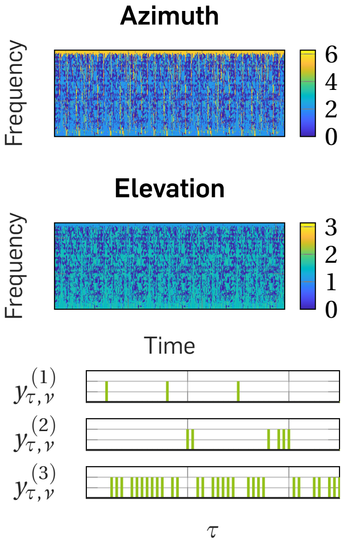

1. Generate DoA time-series for each frequency bin:

$$\boldsymbol{\Theta}_{\nu} = \Big\{ \underbrace{\begin{bmatrix} \phi_{\tau,\nu} & \psi_{\tau,\nu} \end{bmatrix}^{\mathrm{T}}}_{\boldsymbol{\theta}^{\mathrm{T}}_{\tau,\nu}} \Big\}_{\tau=1}^{T}$$

2. Evaluate component-wise Gaussian posteriors:

$$y^{(i)}_{\tau,\nu} = p(\boldsymbol{\theta}_{\tau,\nu} | \boldsymbol{\mu}_i, \boldsymbol{\Sigma}_i)$$

3. Generate time-series from posteriors:

$$\boldsymbol{y}_{\nu} = \{ y^{(i)}_{\tau,\nu} \}_{\tau=1}^{T}$$

Outline

Granger causality test

- Statistical hypothesis test to determine whether a time-series is useful to forecast another.
- Initially proposed and widely used in the context of economics[6].
- Lightweight and computationally efficient framework.
- **Important:** Granger causality does not necessarily imply true causality!

[6] C. W. J. Granger (1969): *"Investigating Causal Relations by Econometric Models and Cross-spectral Methods"*

Granger causality test

- Statistical hypothesis test to determine whether a time-series is useful to forecast another.
- Initially proposed and widely used in the context of economics[6].
- Lightweight and computationally efficient framework.
- **Important:** Granger causality does not necessarily imply true causality!

[6] C. W. J. Granger (1969): *"Investigating Causal Relations by Econometric Models and Cross-spectral Methods"*

Granger causality test

- Statistical hypothesis test to determine whether a time-series is useful to forecast another.
- Initially proposed and widely used in the context of economics[6].
- Lightweight and computationally efficient framework.
- **Important:** Granger causality does not necessarily imply true causality!

[6] C. W. J. Granger (1969): *"Investigating Causal Relations by Econometric Models and Cross-spectral Methods"*

Granger causality test

- Statistical hypothesis test to determine whether a time-series is useful to forecast another.
- Initially proposed and widely used in the context of economics[6].
- Lightweight and computationally efficient framework.
- **Important:** Granger causality does not necessarily imply true causality!

[6] C. W. J. Granger (1969): *"Investigating Causal Relations by Econometric Models and Cross-spectral Methods"*

Granger causality test: algorithm

1. Given two time-series signals $\boldsymbol{x}_\tau$ and $\boldsymbol{y}_\tau$, fit two vector autoregressive (VAR) models

$$\boldsymbol{x}_\tau = \sum_{\mu=1}^{m} \boldsymbol{A}_{\boldsymbol{xx},\mu} \boldsymbol{x}_{\tau-\mu} + \sum_{\mu=1}^{m} \boldsymbol{A}_{\boldsymbol{xy},\mu} \boldsymbol{y}_{\tau-\mu} + \boldsymbol{\epsilon}_{\boldsymbol{x},\tau}, \quad \boldsymbol{\epsilon}_{\boldsymbol{x},\tau} \sim \mathcal{N}(\boldsymbol{0}, \boldsymbol{\Sigma}_{\boldsymbol{x}})$$

$$\boldsymbol{x}_\tau = \sum_{\mu=1}^{m} \boldsymbol{A}'_{\boldsymbol{xx},\mu} \boldsymbol{x}_{\tau-\mu} + \boldsymbol{\epsilon}'_{\boldsymbol{x},\tau}, \quad \boldsymbol{\epsilon}'_{\boldsymbol{x},\tau} \sim \mathcal{N}(\boldsymbol{0}, \boldsymbol{\Sigma}'_{\boldsymbol{x}})$$

2. Construct F-test statistic using the log-likelihood ratio of the residuals

$$\mathscr{F}_{Y \rightarrow X} \equiv \log \left\{ \frac{|\boldsymbol{\Sigma}'_{\boldsymbol{x}}|}{|\boldsymbol{\Sigma}_{\boldsymbol{x}}|} \right\}$$

3. Perform test to evaluate the null hypothesis $H_0 : \boldsymbol{A}_{\boldsymbol{xy},\mu} = \boldsymbol{0} \ \forall \mu$.

Granger causality test: algorithm

1. Given two time-series signals $\boldsymbol{x}_\tau$ and $\boldsymbol{y}_\tau$, fit two vector autoregressive (VAR) models

$$\boldsymbol{x}_\tau = \sum_{\mu=1}^{m} \boldsymbol{A}_{\boldsymbol{x}\boldsymbol{x},\mu} \boldsymbol{x}_{\tau-\mu} + \sum_{\mu=1}^{m} \boldsymbol{A}_{\boldsymbol{x}\boldsymbol{y},\mu} \boldsymbol{y}_{\tau-\mu} + \boldsymbol{\epsilon}_{\boldsymbol{x},\tau}, \quad \boldsymbol{\epsilon}_{\boldsymbol{x},\tau} \sim \mathcal{N}(\boldsymbol{0}, \boldsymbol{\Sigma}_{\boldsymbol{x}})$$

$$\boldsymbol{x}_\tau = \sum_{\mu=1}^{m} \boldsymbol{A}'_{\boldsymbol{x}\boldsymbol{x},\mu} \boldsymbol{x}_{\tau-\mu} + \boldsymbol{\epsilon}'_{\boldsymbol{x},\tau}, \quad \boldsymbol{\epsilon}'_{\boldsymbol{x},\tau} \sim \mathcal{N}(\boldsymbol{0}, \boldsymbol{\Sigma}'_{\boldsymbol{x}})$$

2. Construct F-test statistic using the log-likelihood ratio of the residuals

$$\mathscr{F}_{\boldsymbol{Y}\to\boldsymbol{X}} \equiv \log\left\{\frac{|\boldsymbol{\Sigma}'_{\boldsymbol{x}}|}{|\boldsymbol{\Sigma}_{\boldsymbol{x}}|}\right\}$$

3. Perform test to evaluate the null hypothesis $H_0 : \boldsymbol{A}_{\boldsymbol{x}\boldsymbol{y},\mu} = \boldsymbol{0} \ \forall \mu$.

Granger causality test: algorithm

1. Given two time-series signals $\boldsymbol{x}_\tau$ and $\boldsymbol{y}_\tau$, fit two vector autoregressive (VAR) models

$$\boldsymbol{x}_\tau = \sum_{\mu=1}^{m} \boldsymbol{A}_{\boldsymbol{xx},\mu}\boldsymbol{x}_{\tau-\mu} + \sum_{\mu=1}^{m} \boldsymbol{A}_{\boldsymbol{xy},\mu}\boldsymbol{y}_{\tau-\mu} + \boldsymbol{\epsilon}_{\boldsymbol{x},\tau}, \quad \boldsymbol{\epsilon}_{\boldsymbol{x},\tau} \sim \mathcal{N}(\boldsymbol{0}, \boldsymbol{\Sigma}_{\boldsymbol{x}})$$

$$\boldsymbol{x}_\tau = \sum_{\mu=1}^{m} \boldsymbol{A}'_{\boldsymbol{xx},\mu}\boldsymbol{x}_{\tau-\mu} + \boldsymbol{\epsilon}'_{\boldsymbol{x},\tau}, \quad \boldsymbol{\epsilon}'_{\boldsymbol{x},\tau} \sim \mathcal{N}(\boldsymbol{0}, \boldsymbol{\Sigma}'_{\boldsymbol{x}})$$

2. Construct F-test statistic using the log-likelihood ratio of the residuals

$$\mathscr{F}_{\boldsymbol{Y}\rightarrow\boldsymbol{X}} \equiv \log\left\{\frac{|\boldsymbol{\Sigma}'_{\boldsymbol{x}}|}{|\boldsymbol{\Sigma}_{\boldsymbol{x}}|}\right\}$$

3. Perform test to evaluate the null hypothesis $H_0 : \boldsymbol{A}_{\boldsymbol{xy},\mu} = \boldsymbol{0}\ \forall\mu$.

Pairwise GCT on toy example data

Constructing the Granger matrix and causal graph:

$$\log p\left(\boldsymbol{\theta} \,|\, \{\pi_i, \boldsymbol{\mu}_i, \boldsymbol{\Sigma}_i\}_{i=1}^{C}\right)$$

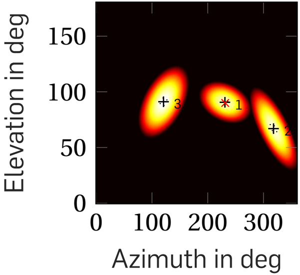

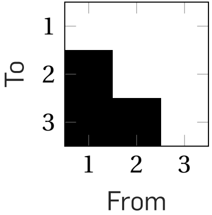

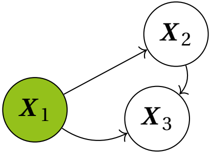

Root node selection using Tarjan's algorithm.[7]

[7] R. Tarjan (1971): *"Depth-first search and linear graph algorithms"*

Outline

Experimental setup

- Simulation study using a single speech source in a reverberant room of size $8\,\mathrm{m} \times 5\,\mathrm{m} \times 3\,\mathrm{m}$ with varying $T_{60} \in \{0.5\,\mathrm{s}, \ldots, 2.5\,\mathrm{s}\}$.
- RIRs for a spherical microphone array with 32 microphones were generated using the image source method.[8]
- Hyperparameter tuning on a dedicated validation set with different speakers, source/array positions and fixed T_{60}.
- Monte Carlo simulations were conducted with 100 runs for each experimental configuration.
- Localization root mean square error (RMSE) was used as evaluation metric.

[8] J. B. Allen, D. A. Berkley (1979): *"Image method for efficiently simulating small-room acoustics"*

Experimental setup

- Simulation study using a single speech source in a reverberant room of size $8\,\mathrm{m} \times 5\,\mathrm{m} \times 3\,\mathrm{m}$ with varying $T_{60} \in \{0.5\,\mathrm{s}, \ldots, 2.5\,\mathrm{s}\}$.
- RIRs for a spherical microphone array with 32 microphones were generated using the image source method.[8]
- Hyperparameter tuning on a dedicated validation set with different speakers, source/array positions and fixed T_{60}.
- Monte Carlo simulations were conducted with 100 runs for each experimental configuration.
- Localization root mean square error (RMSE) was used as evaluation metric.

[8] J. B. Allen, D. A. Berkley (1979): *"Image method for efficiently simulating small-room acoustics"*

Experimental setup

- Simulation study using a single speech source in a reverberant room of size $8\,\mathrm{m} \times 5\,\mathrm{m} \times 3\,\mathrm{m}$ with varying $T_{60} \in \{0.5\,\mathrm{s}, \ldots, 2.5\,\mathrm{s}\}$.
- RIRs for a spherical microphone array with 32 microphones were generated using the image source method.[8]
- Hyperparameter tuning on a dedicated validation set with different speakers, source/array positions and fixed T_{60}.
- Monte Carlo simulations were conducted with 100 runs for each experimental configuration.
- Localization root mean square error (RMSE) was used as evaluation metric.

[8] J. B. Allen, D. A. Berkley (1979): *"Image method for efficiently simulating small-room acoustics"*

Experimental setup

- Simulation study using a single speech source in a reverberant room of size $8\,\mathrm{m} \times 5\,\mathrm{m} \times 3\,\mathrm{m}$ with varying $T_{60} \in \{0.5\,\mathrm{s}, \ldots, 2.5\,\mathrm{s}\}$.
- RIRs for a spherical microphone array with 32 microphones were generated using the image source method.[8]
- Hyperparameter tuning on a dedicated validation set with different speakers, source/array positions and fixed T_{60}.
- Monte Carlo simulations were conducted with 100 runs for each experimental configuration.
- Localization root mean square error (RMSE) was used as evaluation metric.

[8] J. B. Allen, D. A. Berkley (1979): *"Image method for efficiently simulating small-room acoustics"*

Experimental setup

- Simulation study using a single speech source in a reverberant room of size $8\,\mathrm{m} \times 5\,\mathrm{m} \times 3\,\mathrm{m}$ with varying $T_{60} \in \{0.5\,\mathrm{s}, \ldots, 2.5\,\mathrm{s}\}$.
- RIRs for a spherical microphone array with 32 microphones were generated using the image source method.[8]
- Hyperparameter tuning on a dedicated validation set with different speakers, source/array positions and fixed T_{60}.
- Monte Carlo simulations were conducted with 100 runs for each experimental configuration.
- Localization root mean square error (RMSE) was used as evaluation metric.

[8] J. B. Allen, D. A. Berkley (1979): *"Image method for efficiently simulating small-room acoustics"*

Results

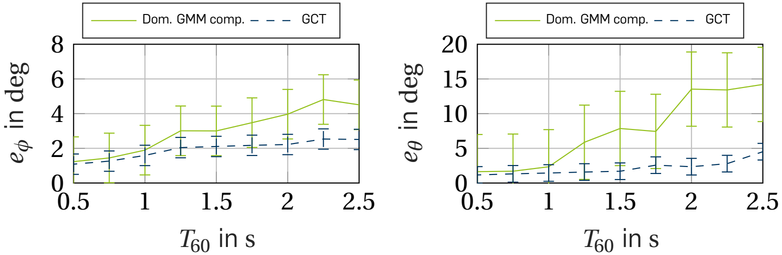

T_{60} in s	0.50	0.75	1.00	1.25	1.50	1.75	2.00	2.25	2.50
Coincidence rate	0.97	0.93	0.91	0.81	0.79	0.79	0.72	0.65	0.65

Coincidence rate represents the degree to which the same DoA components of the GMM were selected by the proposed method and the baseline.

Results

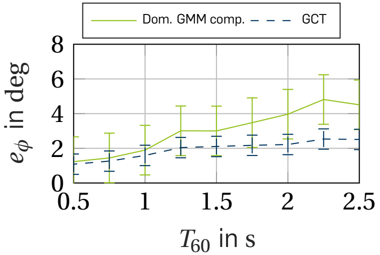

T_{60} in s	0.50	0.75	1.00	1.25	1.50	1.75	2.00	2.25	2.50
Coincidence rate	0.97	0.93	0.91	0.81	0.79	0.79	0.72	0.65	0.65

Coincidence rate represents the degree to which the same DoA components of the GMM were selected by the proposed method and the baseline.

Outline

Outlook

Incorporating temporal context yields significant performance improvements. Still, the current study is a proof-of-concept and many important challenges remain to be solved:

- Extensive hyperparameter tuning is required.
  $\Rightarrow$ *Apply machine learning methods to predict hyperparameters?*
- Method is restricted to static acoustic scenarios. Moving arrays and/or sources can not be handled with the current framework.
  $\Rightarrow$ *Extend model to a dynamical system representation?*
- Gaussian assumption of GCT is violated by DoA time-series signals used in this study.
  $\Rightarrow$ *Adapt GCT to non-Gaussian cases?* [9]

[9] S. Kim, D. Putrino, S. Ghosh, E. N. Brown (2011): *"A Granger Causality Measure for Point Process Models of Ensemble Neural Spiking Activity"*

Outlook

Incorporating temporal context yields significant performance improvements. Still, the current study is a proof-of-concept and many important challenges remain to be solved:

- Extensive hyperparameter tuning is required.
  ⇒ *Apply machine learning methods to predict hyperparameters?*
- Method is restricted to static acoustic scenarios. Moving arrays and/or sources can not be handled with the current framework.
  ⇒ *Extend model to a dynamical system representation?*
- Gaussian assumption of GCT is violated by DoA time-series signals used in this study.
  ⇒ *Adapt GCT to non-Gaussian cases?* [9]

[9] S. Kim, D. Putrino, S. Ghosh, E. N. Brown (2011): *"A Granger Causality Measure for Point Process Models of Ensemble Neural Spiking Activity"*

Outlook

Incorporating temporal context yields significant performance improvements. Still, the current study is a proof-of-concept and many important challenges remain to be solved:

- Extensive hyperparameter tuning is required.
  ⇒ *Apply machine learning methods to predict hyperparameters?*
- Method is restricted to static acoustic scenarios. Moving arrays and/or sources can not be handled with the current framework.
  ⇒ *Extend model to a dynamical system representation?*
- Gaussian assumption of GCT is violated by DoA time-series signals used in this study.
  ⇒ *Adapt GCT to non-Gaussian cases?* [9]

[9] S. Kim, D. Putrino, S. Ghosh, E. N. Brown (2011): *"A Granger Causality Measure for Point Process Models of Ensemble Neural Spiking Activity"*

Outlook

Incorporating temporal context yields significant performance improvements. Still, the current study is a proof-of-concept and many important challenges remain to be solved:

- Extensive hyperparameter tuning is required.
  $\Rightarrow$ *Apply machine learning methods to predict hyperparameters?*
- Method is restricted to static acoustic scenarios. Moving arrays and/or sources can not be handled with the current framework.
  $\Rightarrow$ *Extend model to a dynamical system representation?*
- Gaussian assumption of GCT is violated by DoA time-series signals used in this study.
  $\Rightarrow$ *Adapt GCT to non-Gaussian cases?* [9]

[9] S. Kim, D. Putrino, S. Ghosh, E. N. Brown (2011): *"A Granger Causality Measure for Point Process Models of Ensemble Neural Spiking Activity"*

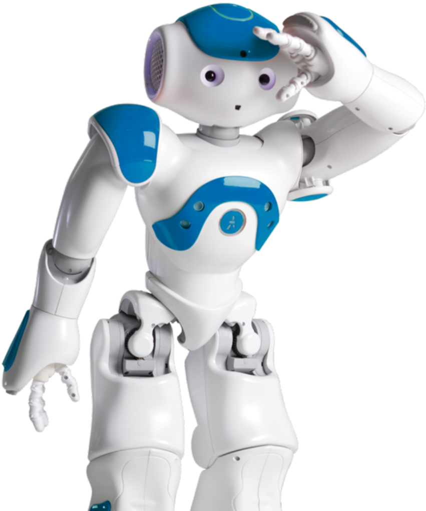

Thank you!